Chemical Engineering Journal 428 (2022) 132607

Contents lists available at ScienceDirect

Chemical Engineering Journal

journal homepage: www.elsevier.com/locate/cej

Gas-shearing synthesis of core–shell multicompartmental microparticles as cell-like system for enzymatic cascade reaction

Qingli Qu [a], Xiaoli Zhang [a], Hossein Ravanbakhsh [c,d], Guosheng Tang [a,c], Jian Zhang [a], Yankang Deng [a], Kevin Braeckmans [b], Stefaan C. De Smedt [a,b], Ranhua Xiong [a], Chaobo Huang [a,*]

[a] Joint Laboratory of Advanced Biomedical Materials (NFU-UGent), College of Chemical Engineering, Nanjing Forestry University (NFU), Nanjing 210037, PR China
[b] Laboratory of General Biochemistry and Physical Pharmacy, Faculty of Pharmaceutical Sciences, Ghent University, 9000 Ghent, Belgium
[c] Division of Engineering in Medicine, Department of Medicine, Brigham and Women's Hospital, Harvard Medical School, Cambridge, MA 02139, United States
[d] Department of Mechanical Engineering, McGill University, Montreal, QC H3A0C3, Canada

ARTICLE INFO

Keywords:
Gas-shearing fabrication
Core–shell multicompartmental microparticles
Mangosteen-like microparticles
Artificial cells
Enzymatic cascade reaction

ABSTRACT

Core-shell multicompartmental microparticles have gained increasing attention as their architecture resembles the multicompartmental composition of eukaryotic cells. However, challenges remain in the fabrication of biocompatible multicompartmental microparticles at a sufficiently high scale. Herein, all-aqueous 'mangosteen-like' core–shell multicompartmental microparticles were created by an oil-free gas-shearing fabrication approach. Both the shell thickness and core size of thus obtained mangosteen-like microparticles can be easily finetuned. Mangosteen-like particles have well segregated (up to eight) compartments which are attractive to precisely control enzymatic cascade reactions. To illustrate the application potential, insulin releasing mangosteen-like microparticles ('artificial pancreatic beta cells') were developed.

1. Introduction

Multicompartmental microparticles may become attractive for many biomedical applications, including 'multidrug delivery' in which different types of drugs are encapsulated in the various compartments of a single particle [1–3]. Also for cell culturing [4–6] for and multi-enzyme tandem reactions, multicompartmental microparticles might become of interest [7,8]. Inspired by the compartmentalized architecture of eukaryotic cells, core–shell multicompartmental microparticles ('synthetic (artificial) cells') have been also created to mimic complex physiological responses in natural cells [9]. For this purpose multi-compartmental microparticles based on coacervates [10], capsosomes [11], vesosomes[12], polymersomes[13] and other hybrid vesicles [14] were investigated. Also phase separation and Pickering emulsions are common methods for fabricating multicompartmental vesicles but major restrictions, including poor control over the properties of the microparticles, remain to exist [15,16]. Microfluidic technologies offer the highest control over the morphology of complex multi-compartmental microparticles [17]. However, since the use of oils and surfactants is inevitably required, such microfluidic techniques might be less suitable for fabricating multicompartmental microparticles as artificial cells [18–20].

Herein, we report an oil-free (all-aqueous), robust, and scalable strategy to produce core–shell multicompartmental ('mangosteen-like') microparticles, with a well-controlled structure, through the use of gas-shearing spray ejector devices (SEDs) (Scheme 1). Briefly, multi-compartmental (two-, four-, six-, or eight-faced) microparticles fabricated by a gas-shearing process in a first SED (SED-A) are pumped into a second SED (SED-B) to become coated, which results in the formation of core–shell multicompartmental microparticles. Segregated and organized compartments in the core of the particles form a unique mangosteen-like structure, which allow for enzymatic cascade reactions. As (biocompatible) biopolymers are believed to be ideal candidates for multicompartment microparticles intended for biomedical use, [21,22] alginate and chitosan were chosen to create the multicompartmental microparticles. It was further demonstrated that the core–shell multi-compartmental microparticles prepared by this strategy are promising to be used as artificial cells. As artificial pancreatic beta cells are believed to be a meaningful strategy for diabetes treatment, we designed core–shell multicompartmental microparticles which can sense a hyperglycemic environment and release insulin.

* Corresponding author.
E-mail address: Chaobo.huang@njfu.edu.cn (C. Huang).

https://doi.org/10.1016/j.cej.2021.132607
Received 30 April 2021; Received in revised form 19 September 2021; Accepted 20 September 2021
Available online 24 September 2021

2. Materials and methods

2.1. Materials

Sodium alginate, chitosan (degree of deacetylation ≥ 95%), anhydrous calcium chloride ($CaCl_2$), glycerophosphate, sodium tripolyphosphate, glucose oxidase, catalase, peroxidase (from horseradish), glucose, insulin, o-phenylenediamine (oPD), Coomassie brilliant blue, dimethyl sulfoxide (DMSO) and 3-(4,5-dimethyl-2-thiazolyl)-2,5-diphenyl tetrazolium bromide (MTT) were all purchased from Aladdin (Shanghai, China). A yellow dye (CWY13150) was purchased from T&H PRIME (Shaoxing, China). Triton x-100, Dulbecco's Modified Eagle's medium (DMEM), and trypsin were acquired from Hyclone Laboratories (Logan, UT, USA). Fetal bovine serum (FBS) was purchased from Sijiqing (Hangzhou, China). Phosphate-buffered saline (PBS) was from Adamas-beta® (Shanghai, China). Calcein acetoxymethyl ester (calcein-AM) / propidium iodide (PI) Double Stain Kit was purchased from Yessen (Shanghai, China). Mouse fibroblast (L929) cells were provided by BioCambridge (Nanjing, China). Mice blood was provided by Kaiji Biotechnology Co., Ltd (Nanjing, China) and collect in accordance with the Regulations on the Administration of Laboratory Animals and national laws, as approved by the Laboratory Animal Ethics Committee at Kaiji Biotechnology Co., Ltd (Nanjing, China) Zebrafish (Danio rerio) were purchased from Lekai Co., Ltd. (Shanghai, China).

2.2. Fabrication of mangosteen-like microparticles

Mangosteen-like microparticles were prepared in two steps making use of SEDs as shown in Scheme 1. First, two-, four-, six-, or eight-faced (core) microparticles were fabricated through the use of a SED-A composed of two-, four-, six-, or eight inner needles (see also Figure S1). Therefore, alginate solutions (2% w/v; in water) which contained fluorescent polystyrene nanoparticles (approximately 0.1% w/v) were pumped into the inner needles (30G-160 μm) using a digital pump (Figure S2). The alginate flow rate was 1 mL/h while the gas flow rate was 5 L/min. To cross-link the alginate droplets into alginate spheres, the droplets were collected in a collecting bath filled with a 2.5% (w/v) $CaCl_2$ solution (solvent water).

To prepare core–shell microparticles, the multicompartmental microparticles were dispersed in an 1% (w/v) alginate solution (solvent water) which was applied in a second SED-B (Scheme 1) and collected in an $CaCl_2$ solution to form mangosteen-like microparticles. The alginate flow rate was 1 mL/h while the gas flow rate was 4 or 6 L/min. Note that in SED-Bs needles with various diameters were used (13G-2000 μm; 14G-1550 μm; 20G-600 μm; 21G-510 μm).

2.3. Fabrication of artificial pancreatic beta cells

In a first step, two-faced microparticles (*i.e.*, Janus microparticles) were prepared as describe in section 2.2; one alginate solution contained glucose oxidase (2 mg/mL) while the second alginate solution contained catalase (1 mg/mL). In the second step, the Janus microparticles were dispersed in an 1% (w/v) chitosan solution (5% acetic acid solution as solvent) in which insulin (5 mg/mL) was dissolved. To solidify the chitosan coating (through ionic cross-linking), the droplets were collected in a collection bath which consisted of an aqueous solution of 50% (w/v) glycerophosphate and 0.5% (w/v) sodium tripolyphosphate.

2.4. Enzymatic cascade reactions in artificial pancreatic beta cells and release of insulin

Freshly prepared (about 50) core–shell (two-faced) microparticles (loaded with glucose oxidase and catalase) were dispersed in 1 mL glucose solution (1 mg/mL or 4 mg/mL glucose in 1 mM PBS as solvent) and incubated at 37 °C. The pH of the glucose solution was measured every 10 min by pH meter (FE28, Mettler Toledo). The release of insulin in the glucose solution was measured using the Coomassie brilliant blue assay (absorption measurements at 595 nm). Experiments were

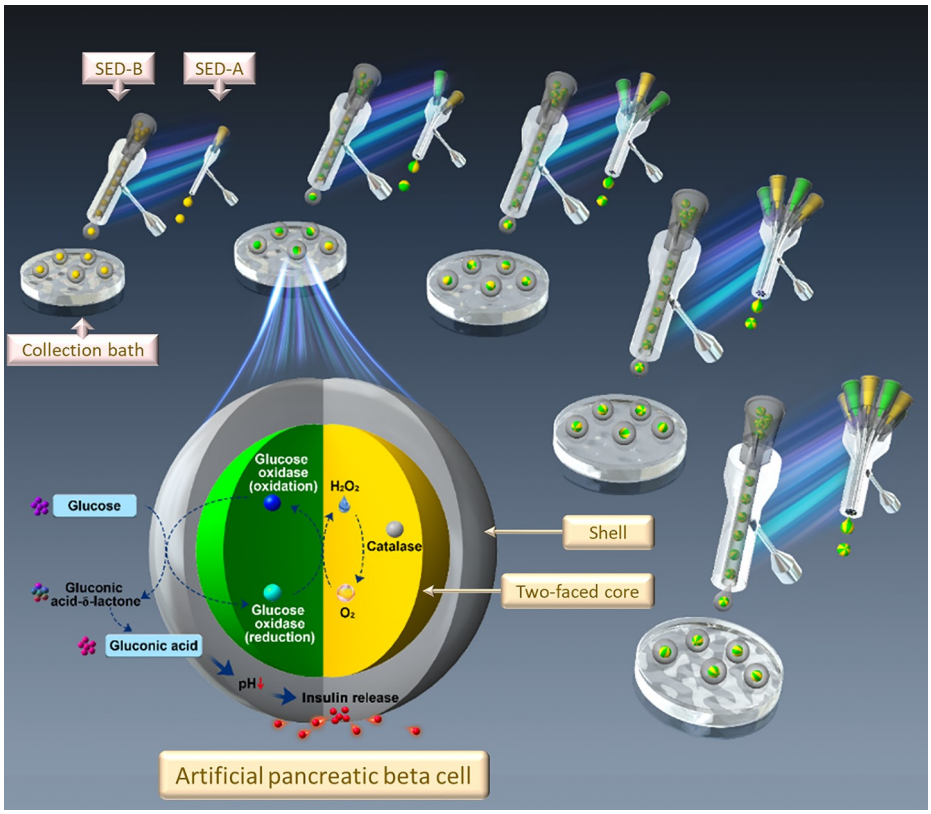

Scheme 1. Schematic illustration of the fabrication of core–shell multicompartmental microparticles though the use of spray ejector devices (SEDs). A first SED (SED-A), is used to fabricate multicompartmental microparticles. In SED-A, inner (liquid-flow) needles are inserted coaxially in an outer needle. The nitrogen gas is transported through the space between the inner needles and the outer needle, generating a shear force allowing the formation of droplets, termed 'gas-shearing'. The number of inner (liquid-flow) needles (*i.e.*, 1, 2, 4 or 8) determines the number of compartments in the microparticles. More details on SED-A were reported previously [23]; see also in Figure S1. A second SED (SED-B) is used to coat the multicompartmental microparticles. As for SED-A, a SED-B is composed of an inner needle coaxially positioned in an outer needle; the multicompartmental microparticles dispersed in the coating solution are pumped through the inner needle; the nitrogen gas is transported through the space between the inner and outer needle, allowing the formation of droplets which are collected in a collection bath where the solidification of the shell occurs. The enlarged microparticle is a two-faced core–shell microparticle which serves as an artificial pancreatic beta cell releasing insulin upon increase in the glucose concentration.

conducted in triplicate, and the results were demonstrated as mean ± SD.

To evaluate whether the microparticle could sustain multiple rounds of enzymatic reactivity, two-faced core–shell microparticles (loaded with glucose oxidase and peroxidase) were suspended in a 4 mg/mL glucose solution (in a lowly concentrated (1 mM) PBS solution) containing oPD (0.2 mg/mL) and incubated for 10 h at 37 ℃ after absorption of the supernatant was measured at 452 nm. Subsequently the microparticles were washed 3 times with deionized water and incubated again in an oPD-glucose solution. This process was repeated 5 times.

3. Results and discussion

3.1. Isotropic microparticles

Initially, isotropic (*i.e.,* one-faced) alginate microparticles were prepared using a SED as illustrated in panel A of Fig. 1. As shown in Fig. 1**B and 1C**, thus obtained microparticles exhibited a normal size distribution (mean size 209 μm, n = 100) with a low polydispersity (SD = 13 μm). The size of the microparticles could be readily controlled by tuning the gas flow rate, as Fig. 1**D** illustrates.

3.2. Core-shell microparticles

Next, the gas-shearing method was employed for fabricating core–-shell microparticles. As shown in Scheme 1 and Fig. 2**A**, isotropic (one-faced) alginate microparticles were suspended in an alginate solution and processed by a SED. The core–shell microparticles shown in Fig. 2**B** were prepared using a 14G needle as the gas flow passage (5 L/min) and a 21G needle for alginate (1 mL/h). It was observed that the core microparticles swelled after the fabrication because of ion-exchange between core microparticles and Na-alginate, and their mean size increased from 209 μm to 240 μm. **Figure S3** shows the stability of microparticles incubated in $CaCl_2$ solution, deionized water, PBS, PBS with 4 mg/mL glucose, and 1% (w/v) alginate solution. Only microparticles suspend in alginate solution swelled, consistent with the above results. Fig. 2**C** show that core–shell microparticles were obtained whose diameter depended on the used needles and gas flow rate. As the cores are rather uniform in size, the varying diameter of the core–shell microparticles indicates that the thickness of the shell could be varied, which might be an attractive feature for their use. As Fig. 2**D** explains, without any modification to the SED, core–shell microparticles with multiple (up to six) cores could be roughly fabricated merely by increasing the concentration of the cores in the alginate solution. Although the number of cores could be relatively well controlled, their spatial distribution within the shell was, however, not controllable. **Figure S4** shows a series of core–shell microparticles containing two cores; they were all fabricated under identical conditions though the position of the cores seemed highly different. As we expected the mutual position of the cores to be important for an accurate regulation of enzymatic cascade reactions, we subsequently aimed to replace the 'multiple cores' by 'a single core composed of multiple compartments', inspired by the structure of mangosteens.

3.3. Mangosteen-like microparticles

In a first stage, as shown in Fig. 3**A**, two-, four-, six-, and eight-faced microparticles were readily produced from an 2% (w/v) alginate solution containing green or red polystyrene nanospheres. The fluorescence intensity profiles, as can be seen in **Figure S5**, indicate that the various compartments within a single microparticle were physically well separated. In the second stage, thus obtained multicompartmental microparticles were processed by an SED to apply an alginate shell. Thereby, mangosteen-like microparticles were obtained, as shown in Fig. 3**B**. As illustrated in Fig. 3**A**, the size of the multicompartmental cores could be precisely controlled upon adjusting experimental parameters. Regardless of the core size, the diameter of the mangosteen-like microparticles remained constant when identical needles and flow rates were used in

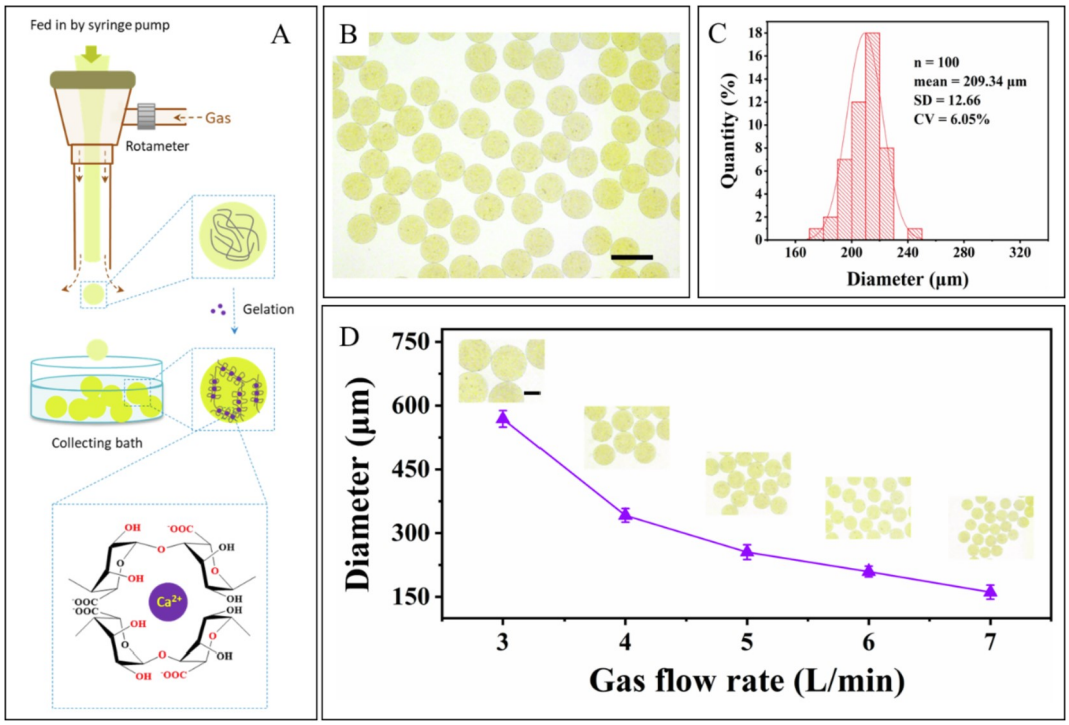

Fig. 1. (A) Fabrication of isotropic (*i.e.*, one-faced) alginate microparticles; the SED consisted of an 30G inner needle (diameter of 160 μm) to transport the yellow dyed alginate solution and an 13G outer needle (diameter of 2000 μm) to transport the nitrogen; the gas flow rate was 6 L/min. (B) Optical image (scale bar is 300 μm) and (C) size distribution of the microparticles. (D) The diameter of the microparticles prepared using different gas flow rates. (For interpretation of the references to colour in this figure legend, the reader is referred to the web version of this article.)

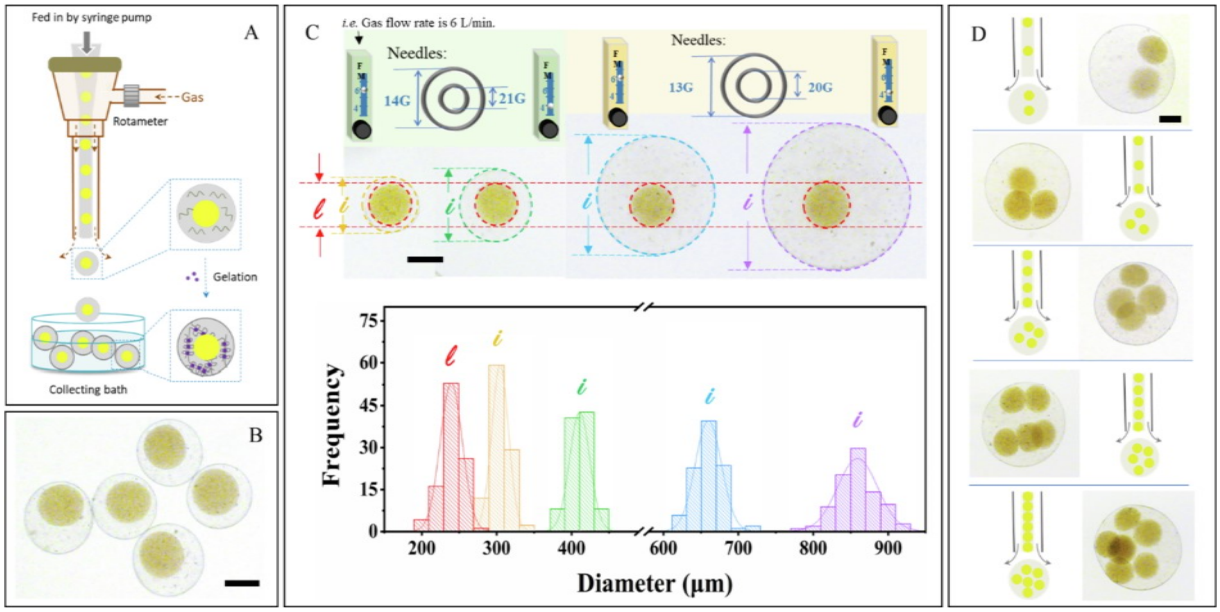

Fig. 2. (A) Fabrication of core–shell microparticles. Isotropic (one-faced) alginate microparticles were dispersed in an 1% alginate solution which was processed by a SED (*i.e.*, SED-B in Scheme 1); thus, both the core (yellow dyed) and shell of the microparticles were composed of alginate. (B) Optical image of core–shell microparticles as obtained using an 21G inner needle (alginate flow rate of 1 mL/h) and an 14G outer needle (gas flow rate of 5 L/min). (C) Size of core–shell microparticles prepared with different needles and using various gas flow rates. (D) Optical images of core–shell microparticles containing multiple cores; the used SED consisted of an 20G inner needle (alginate flow rate of 1 mL/h) and an 13G outer needle (gas flow rate of 4 L/min). The scale bars are 200 μm. (For interpretation of the references to colour in this figure legend, the reader is referred to the web version of this article.)

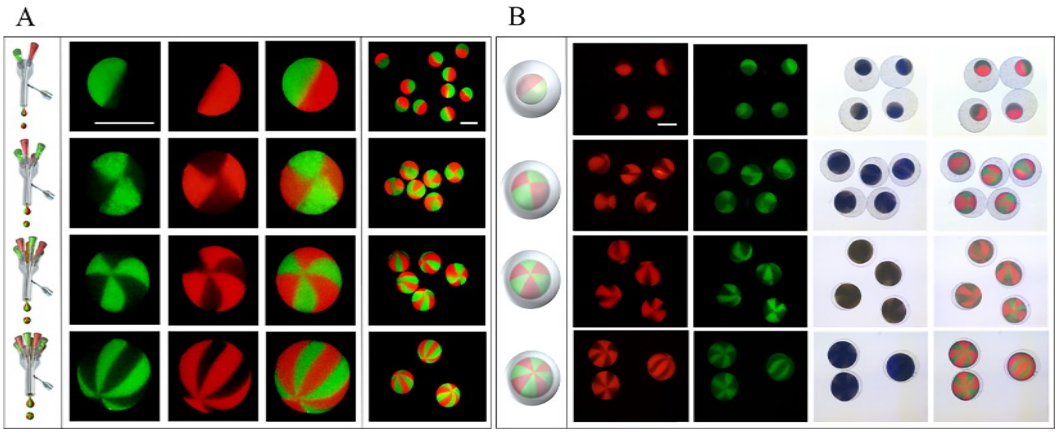

Fig. 3. (A) SEDs used to fabricate multicompartmental alginate microparticles. An 30G inner needle and 10G outer needle was used; the alginate flow rate was 1 mL/h while the gas flow rate equaled 5 L/min. The mean diameter was 362 μm, 438 μm, 457 μm and 521 μm for respectively the two-, four-, six-, and eight-faced microparticles. (B) Microscopy images of (two-, four-, six-, and eight-faced) mangosteen-like microparticles; they were prepared using a 20G inner needle and an 13G outer needle with an alginate and gas flow rate of respectively 1 mL/h and 5 L/min. The mean diameter equaled 728 μm (n = 100); the polydispersity was low (SD = 34 μm).

the coating step; **Figure S6** shows size and size distribution of the mangosteen-like microparticles. **Figure S7** shows that even mangosteen-like microparticles composed of 'multiple multicompartmental cores' could be designed, all illustrating the versatility of the gas-shearing approach.

3.4. Polarization-induced properties

Polarity in natural cells is a common phenomenon caused by the asymmetric configuration of cells, as illustrated in Fig. 4**A**. Many cell activities, such as asymmetric cell division, epithelial and neuronal polarization, chemotactic migration, and cell proliferation, are induced by cell polarization [24–27]. Next, we tested whether mangosteen-like microparticles could express polarities by changing the position of the core. Fig. 4**B** illustrates that the positioning of the core in mangosteen-like microparticles could be tuned though varying the processing conditions (*i.e.,* gas flow rate and diameter of the inner needles) in the coating step. As demonstrated in Fig. 4**B**, the minimal distance between the surface of the core and the shell (denoted as ℓ_{min}) was measured to quantify the polarity; both mangosteen-like microparticles with a perfectly symmetrically positioned core (ℓ_{min}/ℓ equals 1) or a highly asymmetric positioning of the core could be made. An illustration of the microparticle fabrication is shown in Fig. 4**C**; the core reaches its position once the microparticle solidifies in the $CaCl_2$ solution. The force of gravity, viscous stress and interfacial tension are main factors which determine the polarized structure of core–shell microparticles.

Next, we demonstrated the polarization-induced behavior of the core–shell microparticles. Therefore, the alginate cores were made

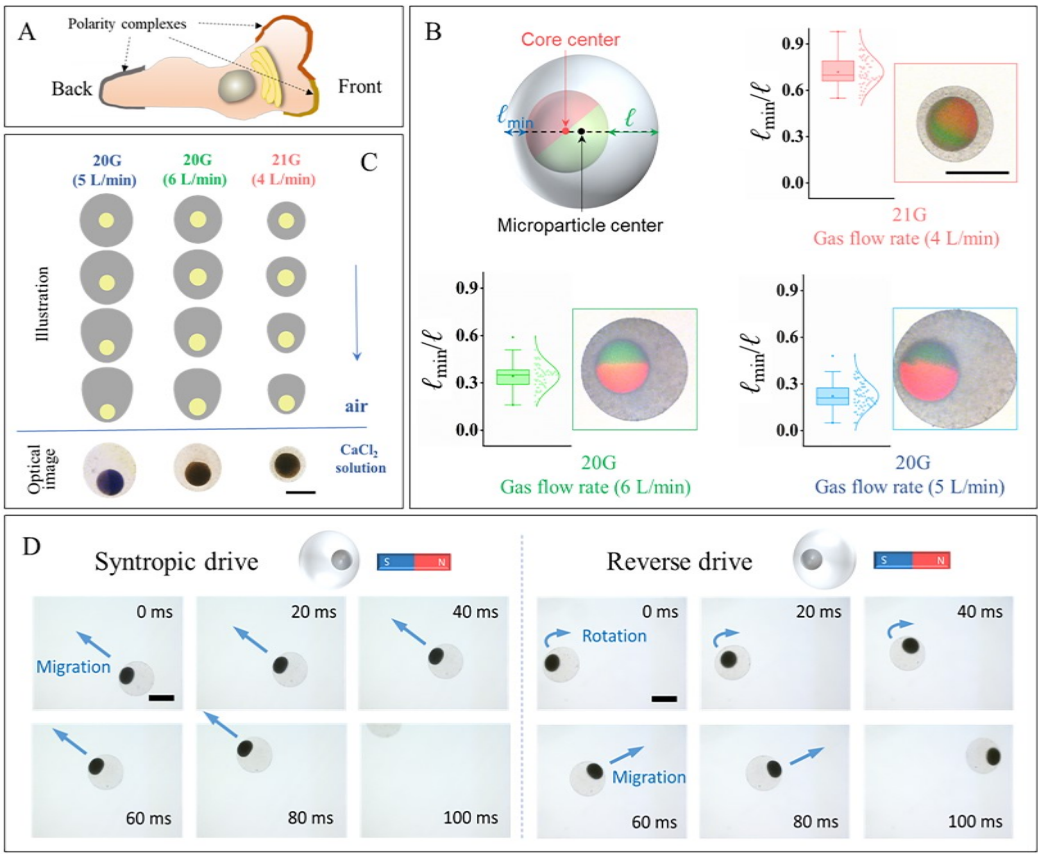

Fig. 4. (A) Schematic illustration of a polarized migratory cell. (B) Positioning of the core: mangosteen-like microparticles were obtained using two-faced cores, the processing conditions in the coating step (*i.e.,* gas flow rate and diameter of the inner needle) were varied. Data were collected from at least 60 microparticles as prepared in three independent experiments. Lines represent mean ± SD. (C) Top: illustration of the fabrication of core–shell microparticles; bottom: optical image of mangosteen-like microparticles; Fe_3O_4 was added to the alginate cores. (D) Time-lapse images of magnetically polarized core–shell microparticles propelled in two different driving modes. The scale bars are 400 μm.

magnetic by adding Fe_3O_4 nanoparticles to the alginate solution (0.4% w/v). Fig. 4**D** and **Video S1** show that polarized core–shell microparticles can crawl, rotate and migrate towards a static magnetic target. The biomimic seeking, orientating and moving behavior was observed in syntropic and reverse drive models. As a control experiment, **Figure S8** shows a non-polarized core–shell microparticle when propelled by a magnet: only a simple translation was observed. The polarization-induced behavior of the core–shell microparticles might be of interest in various applications.

3.5. *Core-shell multicompartmental microparticles as artificial pancreatic beta cells*

Pancreatic beta cells are one of the several cell types in pancreatic islets. Their function is to synthesize and secrete insulin, thereby maintaining glucose homeostasis in the blood. Research shows that diabetes may result from cumulative beta-cell damage induced by sequential environmental insults, and the severity of the diabetes depending on the number of beta cells destroyed [28]. In 2019, International Diabetes Federation claimed that "1 in 11 adults (20–79 years) have diabetes (463 million people)"[29]. Artificial pancreatic beta cells are believed to be a meaningful strategy in diabetes research.

In a next step, as shown in Fig. 5**A**, two-faced alginate cores (Janus cores) were synthesized. Two enzymes, respectively glucose oxidase and catalase, were separately encapsulated in the two compartments of the alginate cores, while insulin was loaded in the chitosan shell. Microscopy images (Fig. 5**A**) and size distribution (Fig. 5**B**) of thus obtained microparticles are shown. Next, we evaluated whether insulin release from thus obtained microparticles could occur upon dispersing the microparticles in glucose solutions. Fig. 5**C** and **Figure S9** show the enzymatic cascade reaction which is expected to occur; glucose (Glu) is expected to be oxidized to gluconic acid by glucose oxidase; the oxidation of Glu leads to the formation of H_2O_2; since excessive H_2O_2 is toxic *in vivo*, the undesired H_2O_2 should be decomposed by catalase to produce O_2; the cascade reaction is completed by reusing the O_2 for glucose oxidation.

Fig. 5**D** shows how the pH change in time upon dispersing the microparticles in glucose solutions; due to the generation of gluconic acid the pH drops from 7.14 to 3.9 in a hyperglycemic solution (4 mg/mL Glu) within 10 h. As seen in Fig. 5**E**, insulin becomes released from the microparticles which we attribute to the protonation of chitosan (pKa ~ 6.5; [30]) which makes the chitosan shell more permeable. To visualize that the enzymatic cascade reactions in the particles last for a substantial time, peroxidase and the chromogenic substrate o-phenylenediamine (oPD, pale yellow) was added to the glucose solution; upon oxidation by peroxidase, oPD forms 2,3-diaminophenazine (DAP, orange) (Fig. 5**F**). As shown in Fig. 5**G**, the microparticles kept on oxidating oPD till the fifth cycle (*i.e.,* refreshing of the medium). It suggests that the artificial cells are rather robust in which enzymatic rations can occur during some time.

3.6. *Biocompatibility of the mangosteen-like microparticles*

Since, in contrast with more traditional microfluidic technologies, oils and surfactants are not used in the gas-shearing process, we expected the mangosteen-like microparticles to be highly cytocompatible. Fig. 6**A** (live/dead staining of cells) and Fig. 6**B** (MTT assay) suggest the artificial pancreatic beta cells, with the biopolymers chitosan and alginate as main components, are minimally cytotoxic. The hemolysis assay, shown in Fig. 6**C**, confirmed the low toxicity of the microparticles. Also in zebrafish, a well-established model for toxicity screening of compounds [31], the microparticles seemed safe as all zebrafish survived the treatment with the microparticle (Fig. 6**D**).

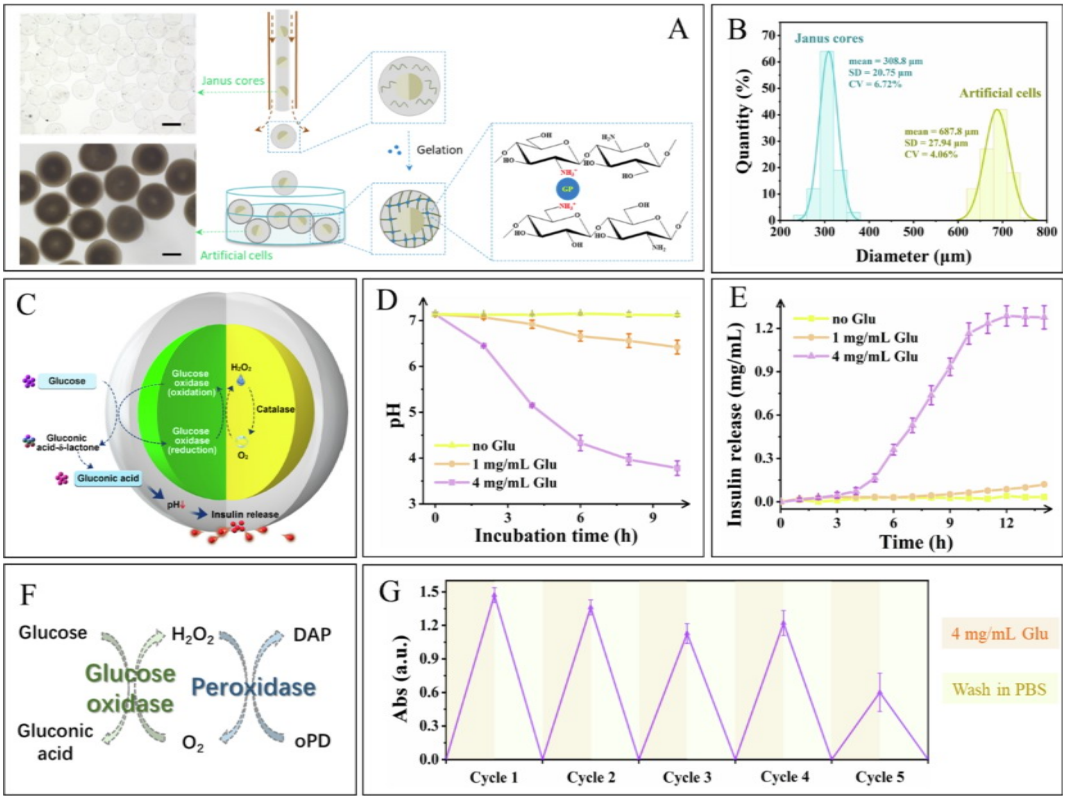

Fig. 5. (A) Fabrication process of artificial pancreatic beta cells. Two-faced (Janus) cores, one compartment loaded with glucose oxidase the other compartment loaded with catalase, were dispersed in a chitosan solution which contained insulin; this dispersion was subsequently processed by a SED; solidification of the chitosan shell occurs through ionic cross-linking in the collection bath. Optical image of respectively the Janus cores (as obtained when using an 30G inner needle (alginate flow rate of 1 mL/h) and an 10G outer needle (gas flow rate of 6 L/min) and the artificial cells (produced using an 20G inner needle (alginate flow rate of 1 mL/h) and an 13G outer needle (gas flow rate of 6 L/min). The scale bars are 300 μm. (B) Size distribution of the Janus cores and artificial cells. (C) Schematic illustration of insulin-release from the microparticles' chitosan shell. (D) Change in pH of the microparticle dispersions containing glucose. (E) Release of insulin in the microparticle dispersions as a function of time. (F) Schematic illustration of the cascade reaction driven by glucose oxidase and peroxidase and the production of DAP upon oxidation of oPD by peroxidase. (G) DAP absorbance (at 452 nm) as observed upon (re-) dispersing the artificial beta cells in glucose solutions (for 5 subsequent cycles).

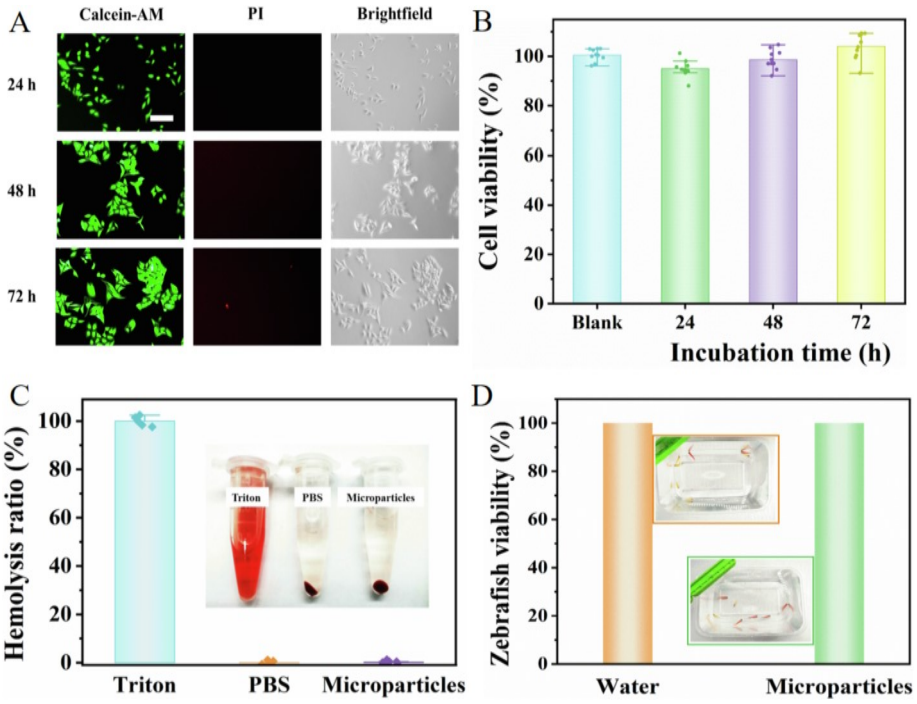

Fig. 6. (A, B) Live/dead staining (A) and cell viability (B) of L929 cells treated with mangosteen-like microparticles for 24 h, 48 h, and 72 h. The scale bar is 200 μm. (C) Hemocompatibility of the mangosteen-like microparticles; according to the ISO 7405:2018, samples are considered hemolytic if the hemolysis ration is > 5% (the hemolysis ratio of the microparticles was 0.27%). (D) Viability and images of zebrafish (inset) in water 7 days (no feeding) with or without the mangosteen-like microparticles.

4. Conclusions and prospects

A robust, scalable strategy, based on the formation of droplets through gas-shearing is presented for the fabrication of core–shell multicompartmental microparticles with a mangosteen-like morphology. As we aim for mangosteen-like to serve as artificial cells, it is attractive that oils and surfactants are not used in the fabrication process, while the particles only contain cytocompatible materials like alginate and chitosan. The all-aqueous fabrication allows precise positioning of the core in the particles, often being a limitation in other fabrication techniques for all-aqueous core–shell microparticles [32]. We showed that enzymes can be separately encapsulated in the segregated compartments of mangosteen-like microparticles. Loading the core of two-faced microparticles with glucose oxidase and catalase, while encapsulating insulin in the shell made of chitosan, resulted in mangosteen-like microparticles which could serve as artificial pancreatic beta cells releasing insulin in hyperglycemic solutions. We foresee that mangosteen-like microparticles might be well suited to allow multiple cascade reactions (for various physiological functions) to occur is in a single microparticle. The mangosteen-like particles reported in this work are rather large which might limit their use *in vivo*. Smaller multicompartmental particles (about 5 μm in size; 'capsosomes'), consisting of multiple liposomes to mimic cell organelles, have been reported [33,34]. It was shown that capsosomes could be internalized and worked in macrophages; they might be suited as a cell implant to support enzymatic activity in cells. Yet, the fabrication procedure seems rather complex. It remains an open question whether the use of much smaller needles and optimized liquid and flow rates will allow to design smaller mangosteen-like microparticles through gas-shearing as reported in this work.

Declaration of Competing Interest

The authors declare that they have no known competing financial interests or personal relationships that could have appeared to influence the work reported in this paper.

Acknowledgments

National Natural Science Foundation of China (No. 21774060), Priority Academic Program Development of Jiangsu Higher Education Institutions (PAPD), and Top-notch Academic Programs Project of Jiangsu Higher Education Institutions (TAPP) are acknowledged with gratitude. We also thank Advanced Analysis & Testing Center, Nanjing Forestry University for the fluorescence microscopy.

Appendix A. Supplementary data

Supplementary data to this article can be found online at https://doi.org/10.1016/j.cej.2021.132607.

References

[1] K. Cho, H.J. Lee, S.W. Han, J.H. Min, H. Park, W.-G. Koh, Multi-compartmental hydrogel microparticles fabricated by combination of sequential electrospinning and photopatterning, Angew. Chem. Int. Ed. Engl. 54 (39) (2015) 11511–11515, https://doi.org/10.1002/anie.201504317.
[2] C.-L. Mou, W. Wang, Z.-L. Li, X.-J. Ju, R. Xie, N.-N. Deng, J. Wei, Z. Liu, L.-Y. Chu, Trojan-horse-like stimuli-responsive microcapsules, Adv. Sci. 5 (6) (2018) 1700960, https://doi.org/10.1002/advs.201700960.
[3] P. Majumder, U. Baxa, S.T.R. Walsh, J.P. Schneider, Design of a multicompartment hydrogel that facilitates time-resolved delivery of combination therapy and synergized killing of glioblastoma, Angew. Chem. Int. Ed. Engl. 57 (46) (2018) 15040–15044, https://doi.org/10.1002/anie.201806483.
[4] T.Y. Lee, R. Praveenkumar, Y.-K. Oh, K. Lee, S.-H. Kim, Alginate microgels created by selective coalescence between core drops paired with an ultrathin shell, J. Mater. Chem. B 4 (19) (2016) 3232–3238, https://doi.org/10.1039/c6tb00580b.
[5] S.-J. Kim, E.M. Kim, M. Yamamoto, H. Park, H. Shin, Engineering multi-cellular spheroids for tissue engineering and regenerative medicine, Adv. Healthc. Mater. 9 (23) (2020) 2000608, https://doi.org/10.1002/adhm.202000608.
[6] J. Wang, Y. Cheng, Y. Yu, F. Fu, Z. Chen, Y. Zhao, Z. Gu, Microfluidic generation of porous microcarriers for three-dimensional cell culture, ACS Appl. Mater. Interfaces 7 (49) (2015) 27035–27039, https://doi.org/10.1021/acsami.5b10442.s001.
[7] R.J.R.W. Peters, M. Marguet, S. Marais, M.W. Fraaije, J.C.M. vanHest, S. Lecommandoux, Cascade reactions in multicompartmentalized polymersomes, Angew. Chem. Int. Ed. Engl. 53 (1) (2014) 146–150, https://doi.org/10.1002/anie.201308141.
[8] H. Wang, Z.e. Zhao, Y. Liu, C. Shao, F. Bian, Y. Zhao, Biomimetic enzyme cascade reaction system in microfluidic electrospray microcapsules, Sci. Adv. 4 (6) (2018) eaat2816, https://doi.org/10.1126/sciadv.aat2816.
[9] K. Zhou, T. Tian, C. Wang, H. Zhao, N. Gao, H. Yin, P. Wang, B.J. Ravoo, G. Li, Multifunctional integrated compartment systems for incompatible cascade reactions based on onion-like photonic spheres, J. Am. Chem. Soc. 142 (49) (2020) 20605–20615, https://doi.org/10.1021/jacs.0c00513.s001.
[10] T. Lu, E. Spruijt, Multiphase complex coacervate droplets, J. Am. Chem. Soc. 142 (6) (2020) 2905–2914, https://doi.org/10.1021/jacs.9b11468.
[11] R. Chandrawati, L. Hosta-Rigau, D. Vanderstraaten, S.A. Lokuliyana, B.S. dler, F. Albericio, a.F. Caruso, Engineering Advanced Capsosomes: Maximizing the Number of Subcompartments, Cargo Retention, and Temperature-Triggered Reaction, ACS Nano 4(3) (2010) 1351–1361. https://doi.org/10.1021/nn901843j.
[12] N.-N. Deng, M. Yelleswarapu, L. Zheng, W.T.S. Huck, Microfluidic assembly of monodisperse vesosomes as artificial cell models, J. Am. Chem. Soc. 139 (2) (2017) 587–590, https://doi.org/10.1021/jacs.6b10977.
[13] P. Wen, X. Wang, S. Moreno, S. Boye, D. Voigt, B. Voit, X. Huang, D. Appelhans, Construction of eukaryotic cell biomimetics: hierarchical polymersomes-in-proteinosome multicompartment with enzymatic reactions modulated protein transportation, Small 17 (7) (2021) 2005749, https://doi.org/10.1002/smll.202005749.
[14] S.S. Yadavalli, Q. Xiao, S.E. Sherman, W.D. Hasley, M.L. Klein, M. Goulian, V. Percec, Bioactive cell-like hybrids from dendrimersomes with a human cell membrane and its components, Proc. Natl. Acad. Sci. U. S. A. 116 (3) (2019) 744–752, https://doi.org/10.1073/pnas.1811307116.
[15] N.G. Moreau, N. Martin, P. Gobbo, T.-Y. Tang, S. Mann, Spontaneous membraneless multi-compartmentalization via aqueous two-phase separation in complex coacervate micro-droplets, Chem. Commun. 56 (84) (2020) 12717–12720, https://doi.org/10.1039/D0CC05399F.
[16] Y. Zhu, Z. Yang, Z. Dong, Y. Gong, Y. Hao, L. Tian, X. Yang, Z. Liu, L. Feng, $CaCO_3$-assisted preparation of ph-responsive immune-modulating nanoparticles for augmented chemo-immunotherapy, Nano-Micro Letters 13 (2020) 29, https://doi.org/10.1007/s40820-020-00549-4.
[17] L.-Y. Chu, A. Utada, R. Shah, J.-W. Kim, D. Weitz, Controllable monodisperse multiple emulsions, Angew. Chem. Int. Ed. Engl. 46 (47) (2007) 8970–8974, https://doi.org/10.1002/anie.200701358.
[18] W. Wang, T. Luo, X.-J. Ju, R. Xie, L. Liu, L.-Y. Chu, Microfluidic preparation of multicompartment microcapsules for isolated co-encapsulation and controlled release of diverse components, Int. J. Nonlinear Sci. Numerical Simulation 13 (5) (2012), https://doi.org/10.1515/ijnsns-2012-0402.
[19] L. Shang, Y. Cheng, J. Wang, H. Ding, F. Rong, Y. Zhao, Z. Gu, Double emulsions from a capillary array injection microfluidic device, Lab Chip 14 (18) (2014) 3489–3493, https://doi.org/10.1039/c4lc00698d.
[20] X. Zhao, Y. Liu, Y. Yu, Q. Huang, W. Ji, J. Li, Y. Zhao, Hierarchically porous composite microparticles from microfluidics for controllable drug delivery, Nanoscale 10 (26) (2018) 12595–12604, https://doi.org/10.1039/c8nr03728k.
[21] A. Gupta, J.L. Terrell, R. Fernandes, M.B. Dowling, G.F. Payne, S.R. Raghavan, W. E. Bentley, Encapsulated fusion protein confers "sense and respond" activity to chitosan-alginate capsules to manipulate bacterial quorum sensing, Biotechnol. Bioeng. 110 (2) (2013) 552–562, https://doi.org/10.1002/bit.24711.
[22] X. Wang, Q. Wang, Enzyme-laden bioactive hydrogel for biocatalytic monitoring and regulation, Acc. Chem. Res. 54 (5) (2021) 1274–1287, https://doi.org/10.1021/acs.accounts.0c00832.
[23] G. Tang, R. Xiong, D. Lv, R.X. Xu, K. Braeckmans, C. Huang, S.C. De Smedt, Gas-shearing fabrication of multicompartmental microspheres: a one-step and oil-free approach, Adv. Sci. 6 (9) (2019) 1802342, https://doi.org/10.1002/advs.201802342.
[24] M. Emmert, P. Witzel, D. Heinrich, Challenges in tissue engineering - towards cell control inside artificial scaffolds, Soft Matter 12 (19) (2016) 4287–4294, https://doi.org/10.1039/c5sm02844b.
[25] W. Hordijk, J. Naylor, N. Krasnogor, H. Fellermann, Population dynamics of autocatalytic sets in a compartmentalized spatial world, Life 8 (3) (2018) 33, https://doi.org/10.3390/life8030033.
[26] D.M. Bryant, K.E. Mostov, From cells to organs: building polarized tissue, Nat. Rev. Mol. Cell Biol. 9 (11) (2008) 887–901, https://doi.org/10.1038/nrm2523.
[27] H. Xie, M. Sun, X. Fan, Z. Lin, W. Chen, L. Wang, L. Dong, Q. He, Reconfigurable magnetic microrobot swarm: Multimode transformation, locomotion, and manipulation, Sci. Robot. 4 (28) (2019) eaav8006, https://doi.org/10.1126/scirobotics.aav8006.
[28] A. Toniolo, T. Onodera, J.-W. Yoon, A.L. Notkins, Induction of diabetes by cumulative environmental insults from viruses and chemicals, Nature 288 (5789) (1980) 383–385, https://doi.org/10.1038/288383a0.
[29] International Diabetes Federation, IDF DIABETES ATLAS Ninth edition (2019) 2019. https://www.diabetesatlas.org/en/resou-rces/.

[30] W. Zhang, X. Jin, H. Li, R.R. Zhang, C.W. Wu, Injectable and body temperature sensitive hydrogels based on chitosan and hyaluronic acid for pH sensitive drug release, Carbohydr. Polym. 186 (2018) 82–90, https://doi.org/10.1016/j.carbpol.2018.01.008.

[31] D. Xiao, J. Cheng, W. Liang, L. Sun, J. Zhao, Metal-phenolic coated and prochloraz-loaded calcium carbonate carriers with pH responsiveness for environmentally-safe fungicide delivery, Chem. Eng. J. 418 (2021) 129274, https://doi.org/10.1016/j.cej.2021.129274.

[32] Q. Qu, J. Zhang, X. Chen, H. Ravanbakhsh, G. Tang, R. Xiong, B.B. Manshian, S. J. Soenen, F. Sauvage, K. Braeckmans, S.C. De Smedt, C. Huang, Triggered release from cellulose microparticles inspired by wood degradation by fungi, ACS Sustainable Chem. Eng. 9 (1) (2021) 387–397, https://doi.org/10.1021/acssuschemeng.0c07514.

[33] M. Godoy-Gallardo, C. Labay, M.M.T. Jansman, P.K. Ek, L. Hosta-Rigau, Intracellular microreactors as artificial organelles to conduct multiple enzymatic reactions simultaneously, Adv. Healthc. Mater. 6 (4) (2017) 1601190, https://doi.org/10.1002/adhm.201601190.

[34] M. Godoy-Gallardo, C. Labay, V.D. Trikalitis, P.J. Kempen, J.B. Larsen, T. L. Andresen, L. Hosta-Rigau, Multicompartment artificial organelles conducting enzymatic cascade reactions inside cells, ACS Appl. Mater. Interfaces 9 (19) (2017) 15907–15921, https://doi.org/10.1021/acsami.6b16275.